Vacas, E. et al. (2013) 'Antitumoral effects of vasoactive intestinal peptide in human renal cell carcinoma xenografts in athymic nude mice', Cancer letters, 336(1), pp. 196–203.

Available at https://doi.org/10.1016/j.canlet.2013.04.033

Antitumoral effects of vasoactive intestinal peptide in human renal cell carcinoma xenografts in athymic nude mice

Eva Vacas [a], M. Isabel Arenas [b], Laura Muñoz-Moreno [a], Ana M. Bajo [a], Manuel Sánchez-Chapado [c,d], Juan C. Prieto [a,*], María J. Carmena [a]

[a] *Department of Systems Biology, Unit of Biochemistry and Molecular Biology, University of Alcalá, 28871 Alcalá de Henares, Spain*

[b] *Department of Biomedicine and Biotechnology, Unit of Cell Biology and Genetics, University of Alcalá, 28871 Alcalá de Henares, Spain*

[c] *Department of Surgery, Medical and Social Sciences, Unit of Surgery, University of Alcalá, 28871 Alcalá de Henares, Spain*

[d] *Department of Urology, Príncipe de Asturias Hospital, 28871 Alcalá de Henares, Spain*

* Corresponding author. Tel.: +34 91 885 4527; fax: +34 91 885 4585.

E-mail address: juancarlos.prieto@uah.es (J.C. Prieto).

Abstract

We studied antitumor effect of VIP in human renal cell carcinoma (RCC) (A498 cells xenografted in immunosuppressed mice). VIP-treated cells gave resulted in p53 upregulation and decreased nuclear β-catenin translocation and NFKB expression, MMP-2 and MMP-9 activities, VEGF levels and CD-34 expression. VIP led to a more differentiated tubular organization in tumours and less metastatic areas. Thus, VIP inhibits growth of A498-cell tumours acting on the major issues involved in RCC progression such as cell proliferation, microenvironment remodelling, tumour invasion, angiogenesis and metastatic ability. These antitumoral effects of VIP offer new therapeutical possibilities in RCC treatment.

Keywords: VIP; MMP; VEGF; NFKB; ccRCC

1. Introduction

The prevalence of renal cell carcinoma (RCC) has increased in recent decades. In the case of localized disease, RCC is curable with surgery, but the prognosis is poor for those patients with distant metastases. In Europe, the majority of patients with RCC have a survival rate of 10% after metastasis [1]. Approximately 30% of patients have metastatic disease at presentation and after complete removal of the primary tumour; a third of the patients will have a recurrence [2]. The histological clear cell subtype (ccRCC) accounts for 80–90% of all RCCs and is characterized by distinct genetic abnormalities. Among them, the loss of function of the von Hippel–Lindau (VHL) tumour-suppressor gene is the most common and is well known for its accompanying hyper vascularity [3]. Clinical trials using antiangiogenic agents proved that these agents are effective for the treatment of RCC [4] but essential research efforts are needed to establish novel molecular-based strategies to improve combat against this aggressive metastatic disease.

The main characteristics of tumoral malignancy are alteration in adhesion, morphology, architecture, and migration capacity. Among a collection of molecular marker for these processes, an important role is attributed to decreased expression of E-cadherin, nuclear localization of β-catenin, activity of matrix metalloproteinases 2 (MMP-2) and 9 (MMP-9), and down-regulation of tumour-suppressor gene p53 [5,6]. In this context, poor survival with a high frequently of metastases in ccRCC is associated with MMP-9 activity [7]. Moreover, VHL protein (pVHL) is a negative regulator of nuclear factor-KB (NFKB): the expression and activity of NFKB are enhanced in the absence of a functional pVHL which results in sustained angiogenesis and a multi-drug resistant RCC phenotype [8]. Also, negative regulation of β-catenin signalling contributes to an aberrantly motile and invasive

tumour cell phenotype [9]. Ultimately, loss of pVHL function may represent a key event in facilitating the development of main aspects of aggressive tumour behaviour. Treatment of advanced RCC continues to be a major challenge for urooncologists. The growth in therapeutic options, largely targeting the VHL/hypoxia-inducible factor (HIF) pathway, has brought improvements in overall and progression-free survival, although durable complete responses remain elusive. Vasoactive intestinal peptide (VIP) is a neuropeptide widely expressed throughout the body and structurally classified as a member of the pituitary adenylate cyclase-activating polypeptide (PACAP)/secretin/glucagon family of peptides. VIP exerts many biological effects that are initiated through PAC_1, $VPAC_1$ and $VPAC_2$ G-protein coupled receptors [10]. A number of laboratories have investigated the role of VIP in key processes that are clearly related such as tumorigenesis, inflammation and immunity among others [10–13]. Available experimental data on the dramatic effects of the neuropeptide in cell lines and animal models of disease support the therapeutical potential of VIP and related peptide analogues in inflammatory and cancer diseases of humans.

We have recently observed the inhibitory effect of VIP on ccRCC proliferation [14] and its leading role in reducing the metastatic progression, increasing ROS levels, and decreasing the activation of NFKB in a VHL-null tumour (A498) human renal epithelial cell line [15]. This cell line expresses quite important levels of VIP and of receptors for this neuropeptide [14,15]. The study of the involvement of VIP in the different steps of the development of the metastatic phenotype in a human ccRCC xenograft model may support the consideration of this neuropeptide as a potential therapeutic tool to alleviate the metastatic capability of these cells. For this purpose, we analyzed VIP effects on different angiogenic and metastatic factors as well as in morphological aspects in a VHL-null tumour (A498 cells) xenograft model.

2. Materials and methods

2.1. Cell culture

The human renal carcinoma cell line was purchased from the American Type Culture Collection ATCC (Rockwell, MD, USA). Cells were cultured in Eagle's Modi- fied Medium supplemented with 10% foetal bovine serum and 1% penicillin/streptomycin/amphotericin B. Cell culture was carried out in a humidified 5% CO_2 environment, at 37 ºC. After reaching 70–80% confluence, cells were washed with PBS, detached with 0.25% trypsin/0.2% EDTA, and plated at 30,000–40,000 cells/ cm^2. The culture medium was replaced every 2 days.

2.2. Animals and preparation of A498 cell xenografts

Athymic nude (nu/nu) 4 weeks-old male mice were obtained from Harlan Iberica (Barcelona, Spain). They were maintained under specific pathogen-free conditions with the approval of the Institutional Animal Care and Use Committee of Alcalá University. Mice were housed at 20 ºC with a 12-h light/dark cycle, and fed autoclaved standard chow and water *ad libitum*. A498 cells were deprived during 24 h, and then incubated for 1 h in the absence or presence of 1 μM VIP (NeoMPS, Strasbourg, France). Afterwards, they were washed with PBS, detached with 25% trypsin/0.2% EDTA, centrifuged at 400*g*, and resuspended in fresh medium. Cells were mixed with Matrigel (BD Bioscence, Madrid, Spain) synthetic basement membrane (1:1, v/v) and then subcutaneously injected in the abdomen (5 x 10^6 cells/ mouse). Six animals were used per group. After sacrifice at 3 weeks of cell injection, tumours were harvested and weighted. Each specimen was divided into three portions: a portion was processed for immunohistochemistry (10% formalin-fixed and paraffin-embedded), and the other portions were frozen in liquid nitrogen and maintained at -80 ºC. The

development of metastases in the whole skeleton was monitored at the end of the experiment by radiography using a Faxitron cabinet X-ray system (Faxitron Bioptics, Tucson, AZ). A semiquantitative scoring was formulated as: 0, no lesions; 1, minor changes; 2, small lesions; 3, significant lesions in bone or lung; and 4, significant lesions in bone and lung. The results represent the average scores from two observers.

2.3. Protein isolation and western blotting

Tumour tissue was homogenized in order to extract the cytosolic and nuclear contents with a commercially available kit (BD Bioscence). Protein content was measured by the Bradford assay using bovine serum albumin (BSA) as a standard. Protein (30 lg) was solubilized in 50 mM Tris–HCl buffer (pH 6.8) containing 10% (v/v) glycerol, 3% (w/v) SDS, 0.01% bromophenol blue, and 0.7 M β-mercaptoethanol. After heating at 95 ºC for 5 min, proteins were resolved by 10% SDS–PAGE and transferred to nitrocellulose sheets (BioTrace/NT, East Hills, NY, USA). Rabbit monoclonal anti-p50 (Santa Cruz Biotechnology, CA, USA) (1:500), anti-p53 (Sigma, Alcobendas, Spain) (1:10,000) and anti-$VPAC_1$-R (Affinity Bioreagents, Golden, CO, USA) (1:10,000), and mouse monoclonal anti-β-catenin (1:2000) (BD Biosciences) antibodies were added followed by incubation for 1 h or overnight. After treatment for 1 h at room temperature with the corresponding HRP-labelled secondary antiserum (BD Biosciences) (1:4000), the signals were detected with enhanced chemiluminiscence reagent (Amersham, Uppsala, Sweden). A β-actin antibody (Merck, Darmstadt, Germany) (1:10,000) was used for loading control.

2.4. RNA extraction and single-step quantitative real-time RT-PCR (QRT-PCR)

Total RNA was extracted from tumour samples using TRI® reagent (Biotech Labs, Houston, TX, USA). QRT-PCR analysis was carried out using RNA samples (90 ng) and SYBRGreen PCR master mix in a one-step RT-PCR protocol (Applied Biosystems, Foster City, CA, USA). The thermal cycling parameters were 30 min at 48 ºC for RT and 10 min at 95 ºC to activate Multiscribe™ Reverse Transcriptase, followed by 50 cycles of 95 ºC for 15 s and 60 ºC for 1 min. ABI-Prism 7000SDS PCR system (Applied Biosystems) was used for PCR reactions with specific primers for CD-44, c-myc, p21 or β-actin. The corresponding sequences of oligonucleotide primers were: CD-44 (sense 5'-AAG GTG GAG CAA ACA CAA CC-3' and antisense 5'-ACT GCA ATG CAA ACT GCA AG-3'); c-MYC (sense 5'-AGC GAC TCT GAG GAG GAA CA-3' and antisense 5'-CTC TGA CCT TTT GCC AGG AG-3'); p21 (sense 5 -ATG AAA TTC ACC CCC TTT CC-3' and antisense 5' -AGG TGA GGG GAC TCC AAA GT-3'); and β-actin (sense 5' -AGA AGG ATT CCT ATG TGG GCG-3' and antisense 5'-CAT GTC GTC CCA GTT GGT GAC). The relative quantification was normalized to β-actin. Results of QRT-PCR were expressed as *Ct* values, where *Ct* is the threshold cycle number at which product is first detected by fluorescence. The amount of target is normalized to an endogenous reference, the housekeeping gene for β-actin. D*Ct* is the difference in *Ct* values derived from the corresponding gene in each sample and b-actin gene. DD*Ct* is the difference between the paired samples. The *n*-fold differential ratio is expressed as 2^{-DDCt}.

2.5. Gelatin zymography

Tumour tissue was homogenized in 50 mM Tris–HCl (pH 7.6) containing 1%

Triton X-100, 200 mM NaCl, 10 mM $CaCl_2$, 0.5 mM phenylmethylsulfonyl fluoride, 2 μg/ml aprotinin, 2 μg/ml leupeptin, 2 μg/ml pepstatin and rotated for 30 min in a cold room. The extract was cleared by centrifugation at 12,000*g* for 20 min at 4 ºC. The samples were analysed by a zymographic technique using 10% SDS–PAGE with 0.1% (w/v) gelatine (Sigma) as the substrate. Each lane was loaded with 6 lg protein and subjected to electrophoresis at 4 ºC. Gels were washed twice in 50 mM Tris (pH 7.4) containing 2.5% (v/v) Triton X-100 for 1 h, followed by two 10-min rinses in 50 mM Tris (pH 7.4). After removal of SDS, the gels were incubated overnight in 50 mM Tris (pH 7.5) containing 10 mM $CaCl_2$, 0.15 M NaCl, 0.1% (v/v) Triton X-100, and 0.02% sodium azide at 37 ºC under constant gentle shaking. Then, the gels were stained with 0.25% Coomasie Brilliant Blue R-250 (Sigma) and de- stained in 7.5% acetic acid with 20% methanol. MMP-2 and 9 activities were semi- quantitatively determined by densitometry of the corresponding bands.

2.6. Determination of vascular endothelial growth factor (VEGF)

VEGF levels were determined in tumour cytosolic extracts by means of an ELISA using the human VEGF DuoSet kit (R&D Systems, Minneapolis, MN) according to the manufacturer's instructions. Data were normalized by the protein concentration in each sample.

2.7. VIP enzyme immunoanalysis (EIA)

VIP levels were determined in tumour homogenates and quantified by EIA with a commercially available kit according to manufacturer‘s instructions (Phoenix Pharmaceutical, Karlsruhe, Germany). The antiserum had 100% cross-reactivity with human and mouse VIP, and <0.02% with PACAP-27.

2.8. Immunohistochemistry

Serial sections, 5-μm-thick, were deparaffinised in xylene and rehydrated using graded ethanol concentrations. Then, they were incubated with 3% hydrogen peroxide for 20 min at room temperature to inactivate endogenous peroxidase. Antigen retrieval was achieved by the pressure cooking method for 2 min in 0.1 M citrate buffer (pH 6). After rinsing in Tris-buffered saline (TBS), the slides were incubated with blocking solution (3% normal donkey serum plus 0.05% Triton in TBS for 45 min to prevent non-specific binding of the first antibody). Afterwards, the sections were incubated, overnight at 4 ºC, with the primary antibody against MMP-2 (1:100), MMP-9 (1:200), and CD-34 (1:100) (Abcam, Cambridge, UK); or E-cadherin (1:500) (Becton Dickinson); in the blocking solution diluted 1:9. Then, the sections were washed in TBS and incubated for 20 min with biotinylated link universal antibody (Dako LSAB® System-HRP, Dako, Glostrup, Denmark). After an extensive wash in TBS, the sections were incubated with streptavidin–peroxidase (Dako) for 20 min at room temperature. The peroxidase activity was detected using the glucose oxidase-DAB-nickel intensification method. DAB stained sections were dehydrated, cleared in xylene, and mounted in DePex (Probus, Badalona, Spain). Sections of tumour samples processed identically, but not incubated with the primary antibody, were used as negative control. As positive controls, sections of human and mouse gut were processed with the same antibody.

2.9. Data analysis

Quantification of band densities was performed using the Quantified One Pro- gram (Bio-Rad). Data shown in the figures are representative at least of three different

experiments. The results are expressed as the mean ± S.E.M. and were statistically treated following the Bonferroni's test for multiple comparisons after one or two-way analysis of variance (ANOVA). The level of significance was set at $p < 0.05$.

3. Results

3.1. Effect of VIP on tumour size and weight

We have previously shown that VIP decreases cell proliferation in the human renal cancer A498 cell line [15]. In the present in vivo study, tumour growth was observed in A498-cell xenografted mice. Interestingly, a group of animals injected with cells that had been pretreated with 1 lM VIP reached a smaller tumour size as compared to the control group (Fig. 1A). Tumours treated with the neuropeptide presented a significant decrease (by 65%) of tumour weight at 3 weeks (Fig. 1B). The analysis of the time taken by the tumour to double its size (TDT) gave values of 2.95 ± 0.09 days in control group and 3.95 ± 0.3 days in VIP-treated group ($p < 0.05$).

3.2. Effect of VIP on metastatic potential of A498 cells

The antimetastatic potential of VIP was evaluated by means of total body radiographies of all mice followed by digital scan in order to evaluate the reduction in the development of metastases. Metastasis was considered positive when there was at least one osteoblastic zone or metastatic nodules in lungs and/or abdominal volume development of the mouse. Control group showed 77% of mice with metastases, while treatment with VIP reduced the number of mice with metastatic areas to 26% (Fig. 1C).

3.3. Effect of VIP on $VEGF_{165}$ expression in A498 tumours

After the screening of the antitumor VIP role in the in vivo development of RCC following A498-cell xenografting, we considered to study the mechanisms that might be involved in this

effect. It is well known that the tumour suppressor protein p53 is inactivated in about half of human cancers [5,6]. For this reason, we determined p53 expression in A498 tumours by western blot. When A498 cells were treated with 1 μM VIP before xenografting, p53 expression in the tumour mass was significantly increased (by 100%) as compared to control conditions (Fig. 2A). We also studied the effect of VIP in p21 gene expression by means of quantitative RT-PCR. In this case, VIP did not modify p21 gene expression in tumour tissue (Fig. 2B).

3.4. Effect of VIP on NFKB (p50) expression in A498 tumours

E-cadherin/b-catenin complex plays an important role in maintaining epithelial integrity. When this complex is altered, the function of β-catenin is not suppressed and it is able to enhance tumour growth. Thus, it is important to analyse the expression of both proteins in order to determine whether VIP treatment is able to modify them. First, we analysed the expression of E-cadherin by immunohistochemistry. Fig. 3A indicates that E-cadherin was not expressed in any of the analysed tumours, either derived from control or VIP-treated A498 cells. Next, we studied the expression of b-catenin by western blot. Fig. 3B shows that nuclear levels of b-catenin in the control group decreased by 50% in the case of cell treatment with the neuropeptide. This downregulatory response could be related with the observation of a similar decrease in the transcription of genes such as c-myc (Fig. 3C) or CD-44 (Fig. 3D), as shown by means of quantitative RT-PCR.

3.5. Expression of tumour VIP and VPAC-1 receptors

MMPs preserve the integrity of extracellular matrix (ECM) by removing undesired proteins; however, over-expressed MMPs play a critical role in tumour invasion and metastasis. In order to study the effect of VIP on MMPs signalling pathway, gelatinolytic

activities were detected by means of gelatine zymography and inmunohistochemistry in A498 tumours. The results showed two bands which must correspond to the latent forms of MMP-2 and MMP-9 (Fig. 4, lower panel). Moreover, these patterns were confirmed by inmunohistochemistry with specific antibodies (Fig. 4, upper panel). Pretreatment of cells with 1 μM VIP significantly decreased both MMP-2 and MMP-9 levels as compared to control group.

3.6. Morphological effects of VIP in A498 tumours

An augmentation in MMP activity is positively linked to increase in metastatic and angiogenic potential of tumours. Since VEGF is a potent angiogenic factor, we investigated the effects of VIP on VEGF165 levels by ELISA. Pretreatment of A498 cells with VIP resulted in a significant antiangiogenic effect in A498 tumours since the neuropeptide decreased by 50% the basal tumour VEGF165 levels (Fig. 5A). In addition to this, we studied the expression of CD-34, a hematopoietic marker of stem cells that recognizes a protein present in endothelial cells. As shown in Fig. 5B, an immunohistochemistry approach showed that treatment of cells with VIP led to decreased CD-34 expression in A498 tumours as compared to control conditions. These results show VIP as a potential inhibitor of angiogenesis.

3.7. Effect of VIP on NF-KB (p50) expression in A498 tumours

In most cancers, the expression of NFKB in cell nucleus is constitutively active. The effect of A498-cell treatment with 1 μM VIP in the nuclear localization of NFKB (p50 subunit) was determined in the corresponding tumours by western blot. Basal nuclear levels of p50 decreased with VIP treatment. Thus, it appears that VIP prevents the translocation of p50 subunit to the nucleus since it was able to reduce by more than 40% the levels of p50 in this

cell compartment (Fig. 6).

3.8. Effect of tumour VIP and VPAC-1 receptors

The reduction of tumour size achieved after a single cell treatment with VIP and the maintenance of the tumour cell antiproliferative response after 3 weeks of mouse xenografting led us to study if the neuropeptide itself could initiate an autocrine/paracrine mechanism after cell treatment. For this purpose, we determined the expression of both VIP and its main receptor, $VPAC_1$, in samples from tumour tissue after 15 days of xenografting animals with cells that had been incubated for 1 h in the absence or presence of 1 μM VIP. Fig. 7A shows the cytosolic levels of VIP, as measured by EIA: VIP levels were about five times higher in tumours treated with the neuropeptide as compared to controls. However, Fig. 7B indicates that the levels of $VPAC_1$ receptors, as measured by western-blot in nuclear extracts from tumours treated with VIP, decreased by 35% under control values; this down-regulatory effect may be conceivably related to the high levels of neuropeptide expression present in VIP treated tumours.

3.9. Morphological effects of VIP in A498 tumours

A detailed analysis of the effect of VIP on A498 cell tumours allowed us to observe morphological changes by immunohistochemistry. The tumour tissue sections did not present a differentiated morphological organization, as seen in the majority of tumour types. In contrast, sections of tumour cells treated with VIP showed an increased number of tubules (Fig. 8), which would mean that the neuropeptide confers characteristics of epithelial cells to the tumour cells. Thus, VIP treatment of A498 cells results in a loss of tumour metastatic ability.

4. Discussion

This study shows the effects of VIP on the expression of molecules involved in the development of renal cell carcinoma. We have previously demonstrated the inhibitory effect of VIP on proliferation, angiogenesis, adhesion, migration and invasion in A498 RCC cells [14,15]. Here we used an *in vivo* xenograft model by injecting nude mice with A498 human renal tumour cells. Two groups were considered: control (untreated cells) and VIP-treated (cells pre- treated for 1 h with 1 μM VIP) tumours. Preliminary observations showed a significant reduction of tumour size after VIP treatment [15]. In the present study, we evaluated both the weight and the molecular characteristics of tumour masses, as well as the meta- static ability in distant areas. Results support that cell treatment with VIP exerts an antiproliferative and antimetastatic role that could represent a new strategy to prevent RCC development. It was noticeable the ability of VIP in giving to the tumour tissue some differentiated morphological organization, as shown by the increase of the number of renal tubules. More remarkable was the important reduction of metastatic areas in animals bearing VIP-treated tumours. The present approximation to the study of tumour metastases was based on X-ray observation of the whole skeleton of xenografted mice. It is only of preliminary nature and merits to be developed by means of a detailed study with different techniques and markers for *in vivo* imaging of tumours.

Since A498 cells express quite important levels of both VIP and VIP receptors [15], the possibility of an autocrine/paracrine action of VIP inside the xenografted tissue may not be discarded. In this context, we have previously observed that the inhibitory effect of VIP upon developing tumours was reverted by using A498 cells that had been preincubated with JV-1-53, a $VPAC_1$-receptor antagonist [15]. Moreover, it is interesting the observation of

sustainable effects of VIP since tumours were removed at 3 weeks after one-single treatment of A498 cells before their subcutaneous implantation. It is conceivably related to the present observation on the important increase of the expression of VIP itself after the initial treatment of A498 cells with the neuropeptide. The finding of five times higher VIP levels as compared to control conditions may explain even the modest (35%) decrease of $VPAC_1$-receptor levels present in tumour extracts derived from VIP-treated cells which may result from a down-regulatory mechanism. We showed in a previous report [15] the time-dependent progression of the tumour mass after xenografting of A498 cells; growth of tumour mass was seen as soon as 2 days after cell injection and it continued until animal sacrifice; cells pretreated with VIP showed a 30% decrease in their ability to develop tumour growth throughout the study.

We have shown in previous studies that VIP exerts tumorigenic effects in human cancers such as prostate [16–18] and breast [19–21] cancers. In these hormone-dependent carcinomas, VIP induces tumour promotion and progression as well as metastases development. However, present results in human renal cell carcinoma xenografts are in apparent conflict with those observations. However, the diversity of VIP-receptor subclasses together with the multiple signals that can result activated after VIP binding conceivably explain the opposite actions of the neuropeptide in different cancer types. Thus, previous data support that VIP mainly activates the cAMP/protein kinase A (PKA) but also the phosphoinositide 3-kinase (PI3-K) and extracellular signal-regulated kinases 1 and 2 (ERK1/2) systems in the growth-stimulatory responses observed in prostate and breast cancers (16–21). On the other hand, the growth-inhibitory response to VIP shown in renal cell carcinoma appears to be mainly related to the cAMP/exchange protein directly activated by cAMP (EPAC/PI3-K) signalling system [14,15]. Previous observations support renoprotective effects of VIP

[14,22]. Thus, we have shown that VIP protected renal proximal tubule HK2 cells against ROS production and oxidative stress damage exerted by H_2O_2 [14]. It should be noted that the increase of free radicals is central to the aetiology of inflammation and other diseases [23] in kidney and other organs. Moreover, clear links exist between the effects of VIP in two pivotal processes such as inflammation and cancer development [10–14,24]. Tumour development goes through different stages. Initiation of tumour is determined by the proliferative ability of tumour cells and p53 can help to pro- mote either the repair and survival of damaged cells or their removal. Sustained stress or irreparable damage induce the killer functions of p53 to activate cell death or senescence [25]. We have determined previously the ability of VIP to decrease the proliferation of A498 RCC cells without causing cell death by apoptosis or necrosis [14,15]. This decrease could be due to deregulation in the expression of cell cycle-related molecules such as p53/p21/ PCNA. In the present study, we demonstrate the ability of VIP to enhance nuclear expression of p53, a molecule closely related to cell cycle progression in A498 cell tumours. This is a promising result, since it is known that the loss of p53 has a dramatic effect achieving tumour development, whereas the reactivation of p53 in tumours from mice lacking the suppressor protein causes a complete tumour regression [5,6,26]. The increased expression of p53 could in turn modify gene expression of p21, a molecule involved in cell cycle arrest in G1 phase. However, present results show that cell treatment with VIP did not elicit any change at this level, which agrees with our previous experiments that indicated that VIP treatment did not caused cell death by apoptosis in A498 cells [15]. On the other hand, the transcription factor NFKB is involved in the regulation of the expression of p53. Present experiments show that VIP led to a significant reduction of nuclear levels of the p50 subunit of NFKB in our *in vivo* model of RCC tumour. In this context, we have previously demonstrated by *in vitro* assays that VIP

treatment resulted in a significant decrease of the high nuclear levels of NFKB that presented the A498 cell line [14]. Other authors working on the relationship between p53 and NFKB have shown that the inhibition NFKB expression leads to death cell by increasing p53 expression [27,28].

Angiogenesis is another pivotal process necessary for tumour progression. The development of a tumour is directly linked to the formation of the formation of new blood vessels which will supply nutrients in order to allow the increase of tumour mass. A key molecule in this field is the vascular endothelial growth factor (VEGF). The expression level of VEGF in RCC is known to strongly correlate with microvessel density, a measure of the degree of angiogenesis [29,30]. However, additional steps are required for vessel formation, including loss of integrity of the extracellular matrix. Tumour xenografts were generated in this study with VHL-negative cells where the basal expression of VEGF must be elevated. We observed an antiangiogenic effect of VIP since it significantly decreased VEGF expression in tumours treated with the neuropeptide. Additionally, VIP also reduced the expression of the endothelial cell marker CD-34. Thus, the neuropeptide might be able to reduce the angiogenic tumoral ability by limiting, in part, the metastatic ability of RCC tumours. In this context, deletion of p53 in glioblastoma cells resulted in overexpression of VEGF which could be normalised by reversing the deletion [31]. It has been observed in VHL-negative CRC cells (A498, 786-O, and RCC4) that p53 expression is independent of VHL, so that VIP may exert a beneficial effect by increasing clear cell carcinoma p53 expression [32].

β-Catenin is an important component of cell–cell adhesion, since it forms part of a dynamic link between E-cadherin and cytoskeleton [33]. In ccCCR, VHL absence can induce cellular invasiveness and loss of E-cadherin. The decreased expression of E-cadherin may

generate the separation of epithelial cells and thus facilitate cell migration [34,35]. Loss of E-cadherin expression occurs in many tumours, including ccRCC, and it is associated with increased b-catenin transcriptional activity and the acquisition of an invasive cell phenotype [36]. Present results show the lack of expression of E-cadherin and the increased nuclear levels of β-catenin in ccRCC tumours. VIP treatment of A498 cells was able to reduce this β-catenin increase which resulted in a lower migratory ability of tumour cells. When β-catenin translocates to the nu- cleus, it binds to members of the Tcf family of transcription factors and modulates the expression of target genes involved in cell proliferation, transformation, and tumour progression, such as c-myc and CD-44 [37,38]. Here, analysis by quantitative real time RT-PCR of c-myc and CD-44 showed that cell treatment with VIP caused a decrease in gene expression related to down-regulation of nuclear β-catenin. Thus, VIP treatment appears to modify tumour progression in ccRCC.

Proteolytic degradation of components of the extracellular matrix and basement membrane facilitates tumour growth, invasion and metastasis. The role of overexpression of MMPs in this process has been firmly established in many classes of human tumours. However, studies on MMP expression in RCCs have been limited [39]. The expression of MMP-2 [40,41] and MMP-9 [42] correlates with advanced stage and poor prognosis in RCC. Our study determined the expression of gelatinases MMP-2 and MMP-9 in A498 RCC xenografts using both gelatin zymography and inmunohistochemistry. We found a significantly downregulation of the expression of MMP-2 and MMP-9 in VIP-treated RCC as compared to controls which was accompanied by a decrease in the invasive capacity of the tumour.

In conclusion, present results show that VIP exerts a potent inhibitory activity on growth

of xenografted renal cell carcinoma A498 cells in athymic nude mice. VIP effects include the main steps of RCC progression such as cell proliferation, angiogenesis, tumour invasion, microenvironment remodelling and metastatic ability in distant areas. This insight into the mechanisms the inhibition of renal carcinoma cell proliferation and migration by VIP adds value for the therapeutical potential of the neuropeptide in this important disease.

Conflict of interest

None declared.

Acknowledgements

This work was supported by the Ministerio de Ciencia e Innovación (Grant SAF2007-63794), Junta de Comunidades de Castilla la Mancha (Grant PII 1/09-0061-3802), Fundación Mutua Madrileña (Grant 2010-002), and Fundación Jesús Serra (Grupo Catalana de Occidente).

References

[1] H. Noble, K. Page, Renal cell cancer: nurses' role in prevention and management, Br. J. Nurs. 21 (2012) S18–S22.

[2] R.J. Motzer, E. Basch, Targeted drugs for metastatic renal cell carcinoma, Lancet 370 (2007) 2071–2073.

[3] M.L. Nickerson, E. Jaeger, Y. Shi, J.A. Durocher, S. Mahurkar, D. Zaridze, V. Matveev, V. Janout, H. Kollarova, V. Bencko, M. Navratilova, N. Szeszenia- Dabrowska, D. Mates, A. Mukeria, I. Holcatova, L.S. Schmidt, J.R. Toro, S. Karami, R. Hung, G.F. Gerard, W.M. Linehan, M. Merino, B. Zbar, P. Boffetta, P. Brennan, N. Rothman, W.H. Chow, F.M. Waldman, L.E. Moore, Improved identification of von Hippel–Lindau gene alterations in clear cell renal tumors, Clin. Cancer Res. 14 (2008) 4726–4734.

[4] L. Li, Y. Gao, L. Zhang, J. Zeng, D. He, Y. Sun, Silibinin inhibits cell growth and

induces apoptosis by caspase activation, down-regulating surviving and blocking EGFR–ERK activation in renal cell carcinoma, Cancer Lett. 272 (2008) 61–69.

[5] D. Bourboulia, W.G. Stetler-Stevenson, Matrix metalloproteinases (MMPs) and tissue inhibitors of metalloproteinases (TIMPs): positive and negative regulators in tumor cell adhesion, Semin. Cancer Biol. 20 (2010) 161–168.

[6] P. Ak, A.J. Levine, P53 and NF-KB: different strategies for responding to stress lead to a functional antagonism, FASEB J. 24 (2010) 3643–3652.

[7] N. Kawata, Y. Nagane, H. Hirakata, T. Ichinose, Y. Okada, K. Yamaguchi, S. Takahashi, Significant relationship of matrix metalloproteinase 9 with nuclear grade and prognostic impact of tissue inhibitor of metalloproteinase 2 for incidental clear cell renal cell carcinoma, Urology 69 (2007) 1049–1053.

[8] C. Morais, G. Gobe, D.W. Johnson, H. Healy, The emerging role of nuclear factor kappa B in renal cell carcinoma, Int. J. Biochem. Cell Biol. 43 (2011) 1537–1549.

[9] B. Peruzzi, G. Athauda, D.P. Bottaro, The von Hippel–Lindau tumor suppressor gene product represses oncogenic beta-catenin signaling in renal carcinoma cells, Proc. Natl. Acad. Sci. USA 103 (2006) 14531–14536.

[10] M. Laburthe, A. Couvineau, V. Tan, Class II G-protein coupled receptors for VIP and PACAP: structure, model of activation and pharmacology, Peptides 28 (2007) 1631–1639.

[11] C. Abad, R.P. Gomariz, J.A. Waschek, Neuropeptide mimetics and antagonists in the treatment of inflammatory disease: focus on VIP and PACAP, Curr. Top. Med. Chem. 6 (2006) 151–163.

[12] R.P. Gomariz, Y. Juarranz, C. Abad, A. Arranz, J. Leceta, C. Martínez, VIP-PACAP system in immunity: new insights for multitarget therapy, Ann. NY Acad. Sci. 1070

(2006) 51–74.

[13] S.G. Smalley, P.A. Barrow, N. Foster, Immunomodulation of innate immune responses by vasoactive intestinal peptide (VIP): its therapeutic potential in inflammatory disease, Clin. Exp. Immunol. 157 (2009) 225–234.

[14] E. Vacas, A.M. Bajo, A.V. Schally, M. Sánchez-Chapado, J.C. Prieto, M.J. Carmena, Vasoactive intestinal peptide induces oxidative stress and suppresses metastatic potential in human clear cell renal cell carcinoma, Mol. Cell. Endocrinol. 365 (2013) 212–222.

[15] E. Vacas, A.B. Fernández-Martínez, A.M. Bajo, M. Sánchez-Chapado, A.V. Schally, J.C. Prieto, M.J. Carmena, Vasoactive intestinal peptide (VIP) inhibits human renal cell carcinoma proliferation, Biochim. Biophys. Acta 2012 (1823) 1676–1685.

[16] A.B. Fernández-Martínez, A.M. Bajo, M. Sánchez-Chapado, J.C. Prieto, M.J. Carmena, Vasoactive intestinal peptide behaves as a pro-metastatic factor in human prostate cancer cells, Prostate 69 (2009) 774–786.

[17] A.B. Fernández-Martínez, A.M. Bajo, M.I. Arenas, M. Sánchez-Chapado, J.C. Prieto, M.J. Carmena, Vasoactive intestinal peptide (VIP) induces malignant transformation of the human prostate epithelial cell line RWPE-1, Cancer Lett. 299 (2010) 11–21.

[18] A.B. Fernández-Martínez, M.J. Carmena, M.I. Arenas, A.M. Bajo, J.C. Prieto, M. Sánchez-Chapado, Overexpression of vasoactive intestinal peptide receptors and cyclooxygenase-2 in human prostate cancer. Analysis of potential prognostic relevance, Histol. Histopathol. 27 (2012) 1093–1101.

[19] A. Valdehita, A.M. Bajo, A.V. Schally, J.L. Varga, M.J. Carmena, J.C. Prieto,

Vasoactive intestinal peptide (VIP) induces transactivation of EGFR and HER2 in human breast cancer cells, Mol. Cell. Endocrinol. 302 (2009) 41–48.

[20] A. Valdehita, A.M. Bajo, A.B. Fernández-Martínez, M.I. Arenas, E. Vacas, P. Valenzuela, A. Ruíz-Villaespesa, J.C. Prieto, M.J. Carmena, Nuclear localization of vasoactive intestinal peptide (VIP) receptors in human breast cancer, Peptides 31 (2010) 2035–2045.

[21] A. Valdehita, M.J. Carmena, A.M. Bajo, J.C. Prieto, RNA interference-directed silencing of VPAC1 receptor inhibits VIP effects on both EGFR and HER2 transactivation and VEGF secretion in human breast cancer cells, Mol. Cell. Endocrinol. 348 (2012) 241–246.

[22] M. Li, J.L. Maderdrut, J.J. Lertora, A. Arimura, V. Batuman, Renoprotection by pituitary adenylate cyclase-activating polypeptide in multiple myeloma and other kidney diseases, Regul. Pept. 145 (2008) 24–32.

[23] D.M. Small, J.S. Coombes, N. Bennet, D.W. Johnson, G.C. Gobe, Oxidative stress, anti-oxidant therapies and chronic kidney disease, Nephrology 17 (2012) 311– 321.

[24] E. González-Rey, N. Varela, A. Chorny, M. Delgado, Therapeutical approaches of vasoactive intestinal peptide as a pleiotropic immunomodulator, Curr. Pharm. Des. 13 (2007) 1113–1139.

[25] K.H. Vousden, C. Prives, Blinded by the light: the growing complexity of p53, Cell 137 (2009) 413–431.

[26] D. Trachootham, W. Lu, M.A. Ogasawara, R.D. Nilsa, P. Huang, Redox regulation of cell survival, Antioxid. Redox Signal. 10 (2008) 1343–1374.

[27] S.I. Grivennikov, M. Karin, Inflammatory cytokines in cancer: tumour necrosis factor and interleukin 6 take the stage, Ann. Rheum. Dis. 70 (Suppl. 1) (2011) i104–i108.

[28] A. Dey, C.S. Verma, D.P. Lane, Updates on p53: modulation of p53 degradation as a therapeutic approach, Br. J. Cancer 98 (2008) 4–8.

[29] H.M. Kluger, S.F. Siddiqui, C. Angeletti, M. Sznol, W.K. Kelly, A.M. Molinaro, R.L. Camp, Classification of renal cell carcinoma based on expression of VEGF and VEGF receptors in both tumor cells and endothelial cells, Lab. Invest. 88 (2008) 962–972.

[30] G. Banumathy, P. Cairns, Signaling pathways in renal cell carcinoma, Cancer Biol. Ther. 10 (2010) 658–664.

[31] S. Reuter, S.C. Gupta, M.M. Chaturvedi, B.B. Aggarwal, Oxidative stress, inflammation and cancer: how are they linked?, Free Radic Biol. Med. 49 (2010) 1603–1616.

[32] N.H. Stickle, L.S. Cheng, I.R. Watson, N. Alon, D. Malkin, M.S. Irwin, M. Ohh, Expression of p53 in renal carcinoma cells is independent of pVHL, Mutat. Res. 578 (2005) 23–32.

[33] M. Vaid, R. Prasad, Q. Sun, K. Katiyar, Silymarin targets b-catenin signaling in blocking migration/invasion of human melanoma cells, PloS One 6 (2011) e23000.

[34] A.J. Evans, R.C. Russell, O. Roche, T.N. Burry, J.E. Fish, V.W.K. Chow, W.Y. Yim, A. Saravanan, M.A. Maynard, M.L. Gervais, R.I. Sufan, A.M. Roberts, L.A. Wilson, M. Betten, C. Vandewalle, G. Berx, P.A. Marsden, M.S. Irwin, B.T. Teh, M.A.S. Jewett, M. Ohh, VHL promotes E2 box-dependent E-cadherin transcription by HIF- mediated regulation of SIP1, and Snail, Mol. Cell. Biol. 27 (2007) 157–169.

[35] W.M. Linehan, J.S. Rubin, D.P. Bottaro, VHL loss of function and its impact on oncogenic signaling networks in clear cell renal cell carcinoma, Int. J. Biochem. Cell Biol. 41 (2009) 753–756.

[36] R.C. Russell, M. Ohh, The role of VHL in the regulation of E-cadherin: a new connectionin an old pathway, Cell Cycle 6 (2007) 56–59.

[37] P. Polakis, The many ways of Wnt in cancer, Curr. Opin. Genet. Dev. 17 (2007) 45–51.

[38] M. Yilmaz, G. Christofori, Mechanisms of motility in metastasizing cells, Mol. Cancer Res. 8 (2010) 629–642.

[39] A. Kugler, B. Hemmerlein, P. Thelen, M. Kallerhoff, H.J. Radzun, R.H. Ringert, Expression of metalloproteinase 2 and 9 and their inhibitors in renal cell carcinoma, J. Urol. 160 (1998) 1914–1918.

[40] M.M. Abdel-Wahed, N.Y. Asaad, M. Aleskandarany, Expression of matrix metalloproteinase-2 in renal cell carcinoma, J. Egypt Natl. Canc. Inst. 16 (2004) 168–177.

[41] T. Sumi, T. Nakatani, H. Yoshida, Y. Hyun, T. Yasui, Y. Matsumoto, E. Nakagawa, K. Sugimura, H. Kawashima, O. Ishiko, Expression of matrix metalloproteinases 7 and 2 in human renal cell carcinoma, Oncol. Rep. 10 (2003) 567–570.

[42] N.H. Cho, H.S. Shim, S.Y. Rha, S.H. Kang, S.H. Hong, Y.D. Choi, S.J. Hong, S.H. Cho, Increased expression of matrix metalloproteinase 9 correlates with poor prognostic variables in renal cell carcinoma, Eur. Urol. 44 (2003) 560–565.

Figure legends

Fig. 1. VIP effect on tumour growth in A498 ccRCC xenografts. A498 cells were incubated for 1 h in the absence or presence of 1 μM VIP, mixed with Matrigel, and subcutaneously injected in nude mice. (A) Inhibition of ccRCC tumour weight by VIP in xenografts. A representative experiment after 21 days of cell injection is shown. (B) After sacrifice at 21 days, tumours were removed for weight measurement. Data are the mean ± S.E.M. of at least three experiments, *** $p < 0.001$ versus control. (C) Metastatic ability: representative X-ray images of whole body of animals with tumours derived from control and VIP-treated cells.

Fig. 2. Effect of 1 μM VIP on p53 nuclear levels (A) and p21 expression (B) in A498 ccRCC xenografts. (A) p53 nuclear levels were measured by western blot. Results were normalized with β-actin. (B) Expression of p21 mRNA in A498 ccRCC xenografts as studied by real-time RT-PCR. All preparations were normalized according to the expression of β-actin mRNA. Data are the mean ± S.E.M. of at least three experiments, ** $p < 0.01$.

Fig. 3. Effect of 1 μM VIP on E-cadherin (A), β-catenin (B), c-myc (C) and CD-44 (D) expression in A498 ccRCC xenografts. (A) Inmunolabelling with E-cadherin antiboby. In control tissues, the labelling was observed in the cytoplasm whereas VIP-treated xenografts did not show immunostaining. Right: microphotograph showing a positive immunoreaction to E-cadherin antibody in the plasma membrane of epithelial cells. Original magnification x300. (B) Nuclear expression of β-catenin by western blot. Expression levels were normalized with β-actin. (C and D) Expression of c-myc and CD-44 mRNA, respectively, in A498 ccRCC xenografts

as studied by real-time RT-PCR. All preparations were normalized according to the expression of β-actin mRNA. Data are the mean ± S.E.M. of at least three experiments ** $p < 0.01$; *** $p < 0.001$.

Fig. 4. Study of the expression of MMP-2 and MMP-9 by inmunohistochemistry (upper panels) and gelatine zimography (lower panels) in A498 ccRCC xenografts. Original magnification x300. A representative experiment is shown. Data are the mean ± S.E.M. of at least three experiments; *** $p < 0.001$, * $p < 0.05$.

Fig. 5. Effect of 1 μM VIP on the expression of VEGF (A) and CD-34 (B) in A498 ccRCC xenografts. (A) $VEGF_{165}$ cytosolic levels were measured by ELISA. The bar diagrams represent the mean ± S.E.M. of three experiments; ** $p < 0.01$ compared with Control. (B) CD-34 expression was measured by immunohistochemistry. Original magnification x300. A representative experiment is shown.

Fig. 6. Effect of 1 μM VIP on p50 nuclear expression in A498 ccRCC xenografts. A representative experiment is shown. Expression levels were normalized with b- actin. The bar diagrams represent the mean ± S.E.M. of three experiments; ** $p < 0.01$ compared with control.

Fig. 7. Effect of VIP on its own expression and VPAC1-receptor (VPAC1-R) expression in human renal tumours. Tumour extracts were prepared after 15 days of xenografting animals with cells that had been incubated for 1 h in the absence or presence of 1 μM VIP. (A) VIP expression was estimated by measuring the cytosolic levels of VIP by EIA. (B) Western-blot of VPAC1-R in nuclear extracts. A representative experiment is shown. Data are the mean ± S.E.M. of at least three experiments; ** $p < 0.01$, *** $p < 0.001$.

Fig. 8. Microphotographs of haematoxylin and eosin sections from A498 ccRCC

xenografts derived from control and VIP-treated cells. Magnification x300. A representative experiment is shown.

Figure 1

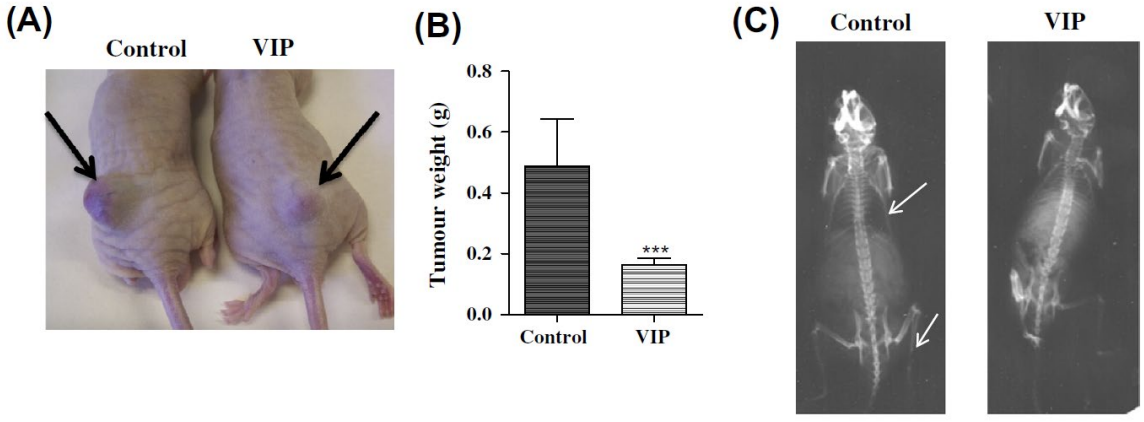
(A)
Control
VIP
(B)
Tumour weight (g)
0.8
0.6
0.4
0.2
0.0
***
Control
VIP
(C)
Control
VIP

Figure 2

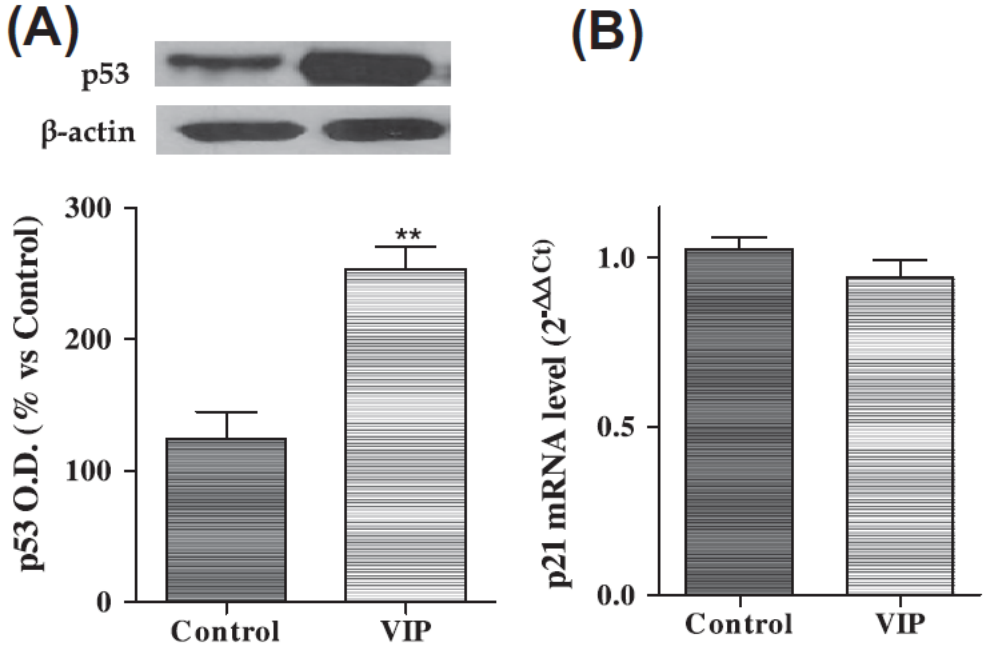
(A)
p53
β-actin
p53 O.D. (% vs Control)
300
200
100
0
**
Control
VIP
(B)
p21 mRNA level (2-ΔΔCt)
1.0
0.5
0.0
Control
VIP

Figure 3

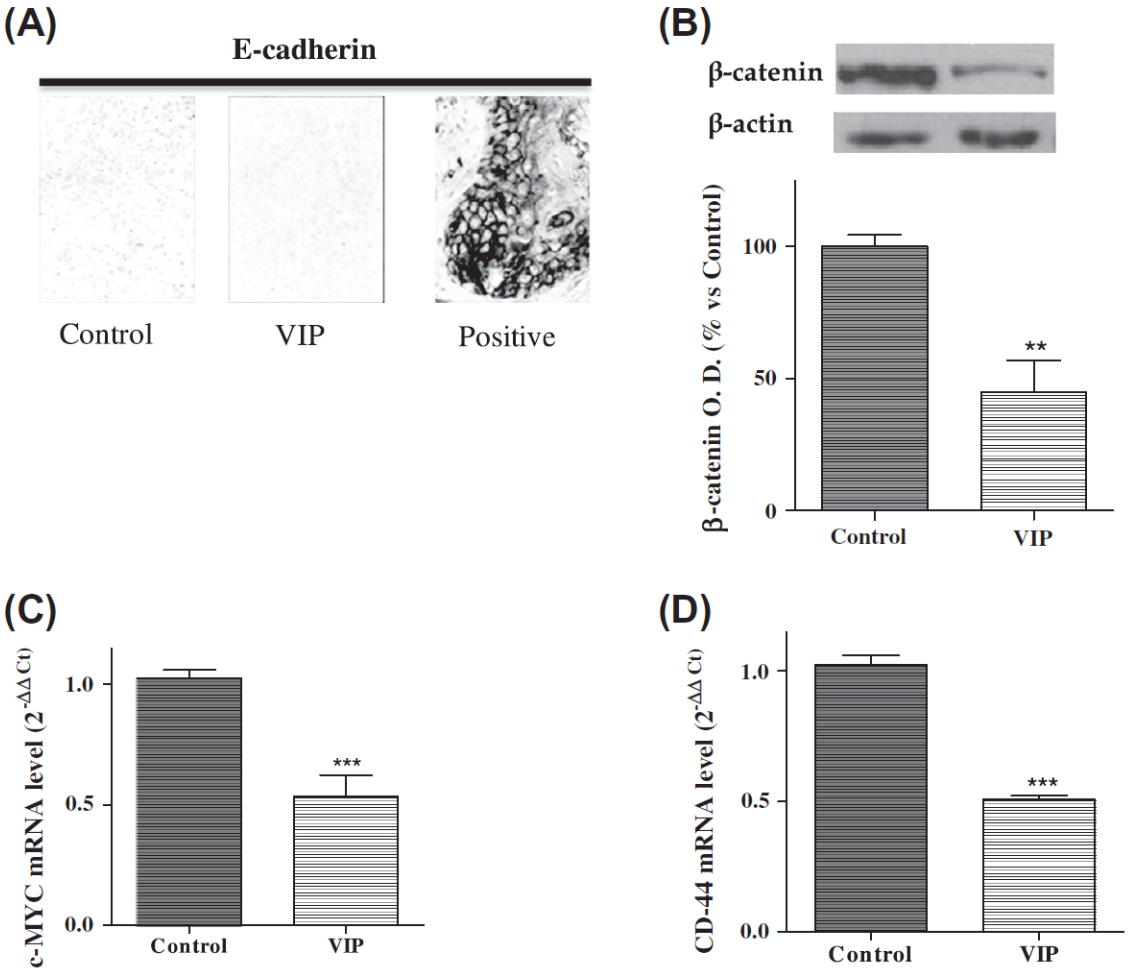
(A)
E-cadherin
Control
VIP
Positive
(B)
β-catenin
β-actin
β-catenin O. D. (% vs Control)
100
50
0
**
Control
VIP
(C)
c-MYC mRNA level (2-ΔΔCt)
1.0
0.5
0.0
***
Control
VIP
(D)
CD-44 mRNA level (2-ΔΔCt)
1.0
0.5
0.0
***
Control
VIP

Figure 4

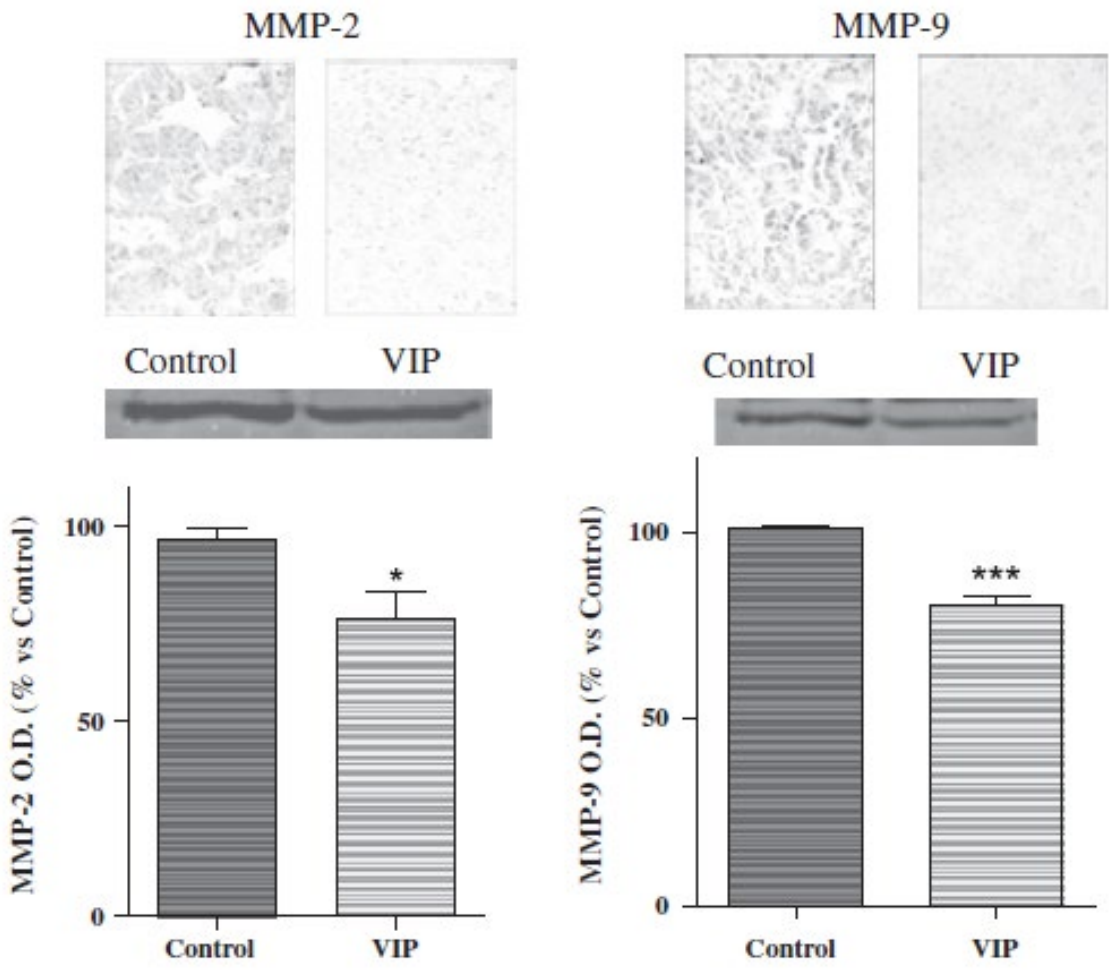
MMP-2
MMP-9
Control
VIP
Control
VIP
MMP-2 O.D. (% vs Control)
MMP-9 O.D. (% vs Control)
100
50
0
*
***
Control
VIP
Control
VIP

Figure 5

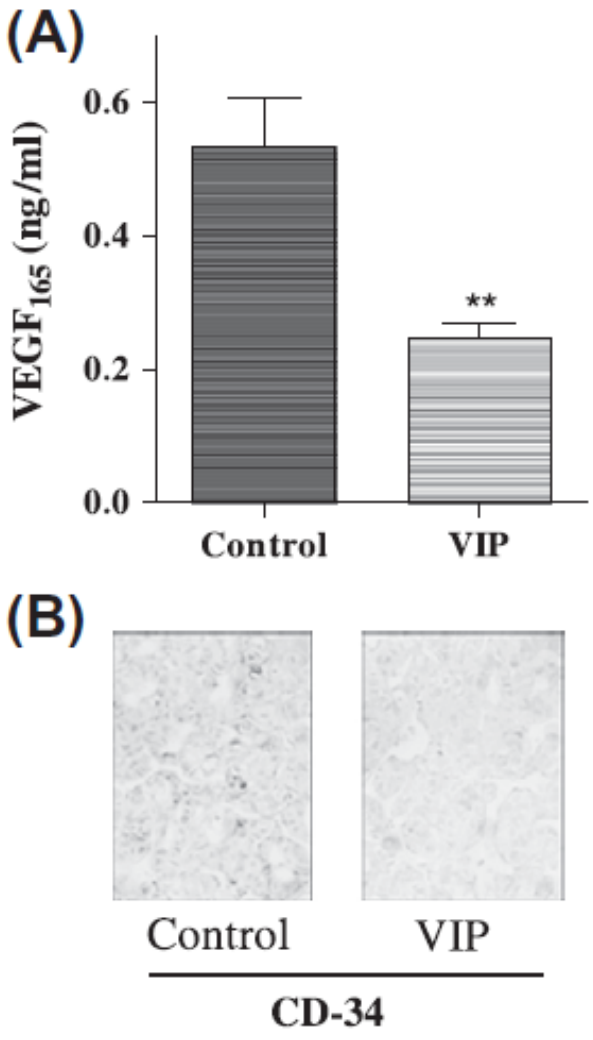

Figure 6

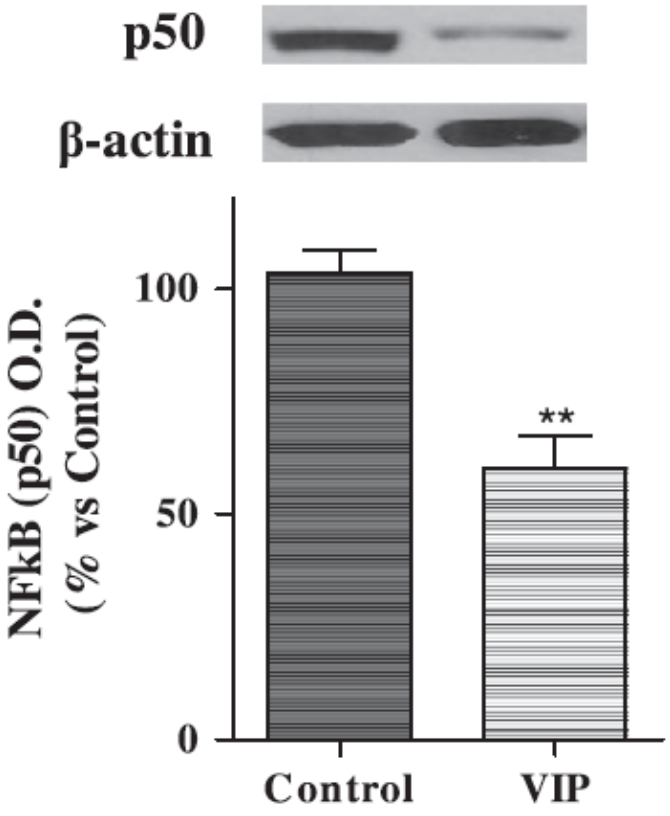

Figure 7

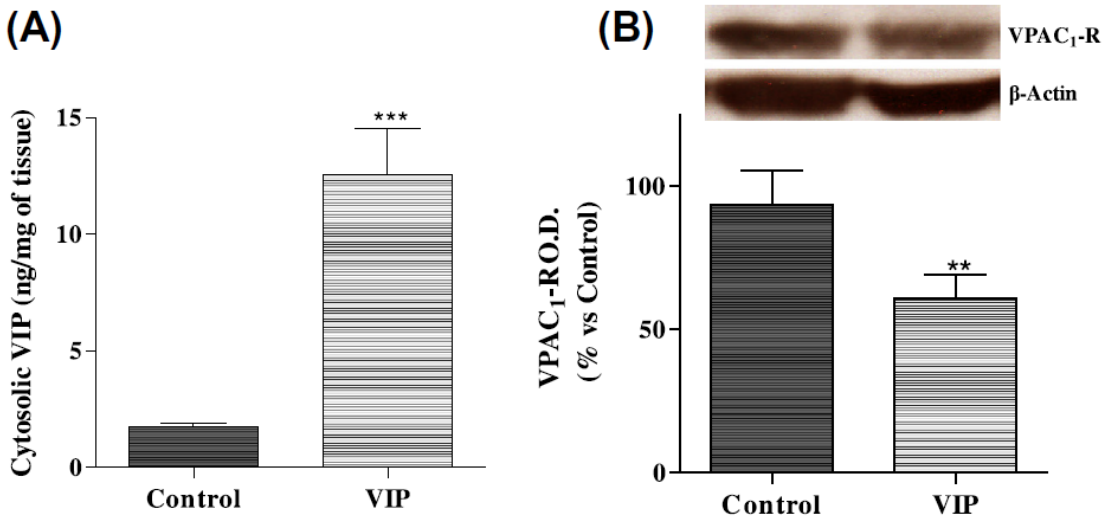
(A)
Cytosolic VIP (ng/mg of tissue)
15
10
5
0
***
Control
VIP
(B)
VPAC1-R
β-Actin
VPAC1-R O.D.
(% vs Control)
100
50
0
**
Control
VIP

Figure 8